FLUID DYNAMIC CHARACTERISTICS OF A FLOATING OBJECT MEASURED BY A MAGNETIC SUSPENSION AND BALANCE SYSTEM

Hiroyuki Fujiwara
National Defense Academy, Department of Mechanical Engineering
1-10-20 Hashirimizu, Yokosuka, Kanagawa, Japan, 239-8686
hiroyuki@nda.ac.jp

Yosuke Mizokami
National Defense Academy, Department of Mechanical Engineering
1-10-20 Hashirimizu, Yokosuka, Kanagawa, Japan, 239-8686

Osami Matsushita
National Defense Academy, Department of Mechanical Engineering
1-10-20 Hashirimizu, Yokosuka, Kanagawa, Japan, 239-8686
osami@nda.ac.jp

ABSTRACT

A Magnetic Suspension and Balance System (MSBS) provides the electromagnetic and non-contact support of a model in a wind tunnel to measure fluid-induced forces[1]-[7]. The purpose of this study is to measure the fluid-induced dynamic coefficients of an object suspended in fluid using the MSBS. We would like to propose a method for determining the effect of the fluid-induced dynamic coefficients by comparing the experimental results of the open-loop transfer function with the numerically simulated ones. In order to show the effectiveness of this method, we measured fluid-induced dynamic coefficients by exciting an object magnetically supported in water.

1. INTRODUCTION

The number of fluid-related machines, such as gas turbines, pumps, and bearings, is used. As their efficiency and accuracy are being improved, it is more important to preliminarily analyze the effect of fluid-induced forces. Particularly, changes in the dynamic characteristics of an object in fluid are difficult to understand in the design stage, which may cause unexpected damage or breakdown of the machines. The above notwithstanding, most researchers experiment and numerically analyze the fluid-induced forces in a statically balanced state, and there are few papers focusing on the dynamic characteristics of an object in fluid.

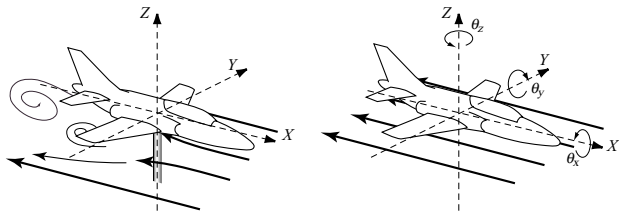

(a) Mechanical support (b) Magnetic support
Figure 1: Support system

In this study, we employed a Magnetic Suspension and Balance System (MSBS) to measure the dynamic characteristics. As shown in Figure 1, the MSBS supports an object in fluid magnetically rather than mechanically to measure the fluid-induced forces without the influence of any supporting rod. The MSBS can also move the floating object electromagnetically to measure the dynamic coefficients. The purpose of this paper is to clarify the effect of the fluid-induced forces on the dynamic coefficients of the object by measuring the open-loop transfer function of a feedback control system used for magnetic levitation, and comparing the experimental results with the simulated ones. This paper outlines a fabricated system and describes results from the measurement of the dynamic coefficients of an object in water as a fundamental experiment.

2. NDA-MSBS

2.1 System summary

Figure 2 illustrates the MSBS fabricated. We built this testing system based on a MSBS developed by Fukuoka Institute of Technology (FIT)[7]. Since our MSBS employs permanent magnets for levitation, it is not necessary to flow a large current through electromagnets for control (Figure 2). Only one permanent magnet is arranged in the upper part of the test equipment. The model is basically supported by making the gravity acting on it equal to the attractive force between the permanent magnets of the equipment and the model, and the elevation of the model is mainly controlled by a special coil installed directly below the equipment's permanent magnet. Moreover, the attitude of the model is controlled by eight coils arranged in the upper and lower portions. The model has six degrees of freedom: the x, y, and z translations as well as the θ_x, θ_y, and θ_z rotations. This experimental system can control five degrees of

freedom except θ_z.

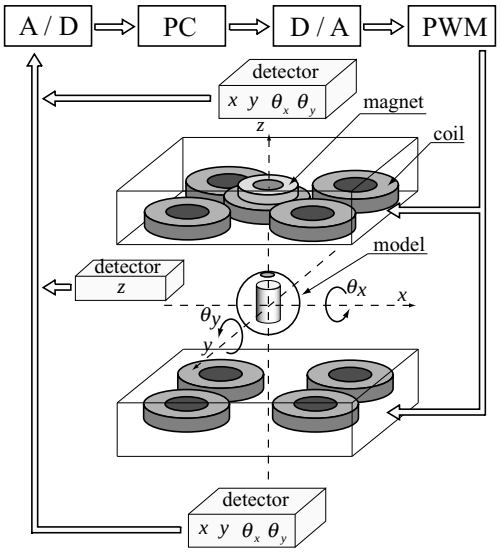

Figure 2: NDA-MSBS
(40-by-40-cm wind tunnel experimental system)

2.2 SENSING SYSTEM

In order to detect the motions *x, y,* θ_x, and θ_y, we put reflective stickers on the top and bottom surfaces of the model and led a laser beam to them as shown on the left side of Figure 3. The reflected beam is deflected again from a half mirror (a transmission factor of 50 percent) and goes to a detector having an array of four photo diodes. The detector gives the moving distance and direction of the beam. Arranging this laser-detector system on the upper and lower sides of the model measures the displacement and tilt of the model. In the z axis, we emitted another laser beam to the top of the model and adjusted the laser position so that the beam was blocked according to the z displacement of the model. The variation in the intensity of the laser beam on the detector is proportional to the model's displacement in the z direction.

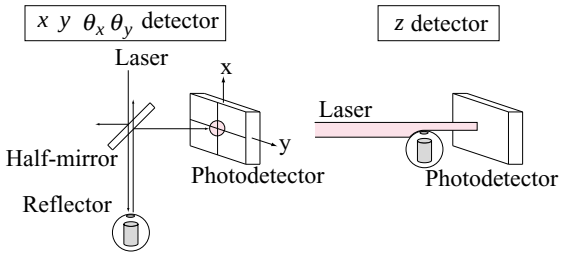

Figure 3: Sensor

2.3 MAGNETIC FIELD AND FORCE

2.3.1 Magnetic field generated by an air-core coil

Let us examine the flux density $\boldsymbol{B}$ at an arbitrary point in a magnetic field induced by a circular current. Letting $\mathrm{d}I$ be a small current flowing through the point q on the circle having the radius r as shown in Figure 4, Biot-Savart law gives the flux density $\mathrm{d}\boldsymbol{B}$ at the point p as follows:

$$\mathrm{d}\boldsymbol{B} = \frac{\mu_0 \mathrm{d}I}{4\pi R^2} \qquad (1)$$

where μ_0 is the absolute permeability of vacuum, $\mathrm{d}I$ is the small current, and R is the distance between the points p and q.

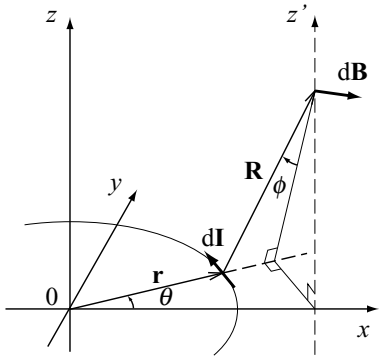

Figure 4: $\mathrm{d}\boldsymbol{B}$ for Coil

Meanwhile,

$$\mathrm{d}I = Ir\mathrm{d}\theta \qquad (2)$$

Substituting this equation into Equation (1) gives

$$\mathrm{d}\boldsymbol{B} = \frac{\mu_0 Ir\mathrm{d}\theta}{4\pi R^2} \qquad (3)$$

The flux density $\boldsymbol{B}$ at the point p is given by integrating the equation above along the circumference of the circle. Accordingly,

$$\boldsymbol{B} = \int_0^{2\pi} \frac{\mu_0 Ir\mathrm{d}\theta}{4\pi R^2} \qquad (4)$$

The x, y, and z components are represented respectively as

$$\boldsymbol{B}_x = \int_0^{2\pi} \frac{\mu_0 Ir\mathrm{d}\theta}{4\pi R^2} \cos\phi\cos\theta \qquad (5)$$

$$\boldsymbol{B}_y = \int_0^{2\pi} \frac{\mu_0 Ir\mathrm{d}\theta}{4\pi R^2} \cos\phi\sin\theta \qquad (6)$$

$$\boldsymbol{B}_z = \int_0^{2\pi} \frac{\mu_0 Ir\mathrm{d}\theta}{4\pi R^2} \sin\phi \qquad (7)$$

If the point p sits on the $x-z$ plane, the coil is symmetrical to the x axis, resulting in $\boldsymbol{B}_y = 0$.

2.3.2 Force acting on the model

A force acting on the model in the magnetic field is given by the tilt of the magnetic field and the magnetic moment of the magnet installed in the model. Namely, it is represented as the following equations:

$$\boldsymbol{F} = (M \cdot \nabla)\boldsymbol{H} \qquad (8)$$

$$M = B_r V \qquad (9)$$

where $\boldsymbol{H}$ is the intensity of magnetic field ($\boldsymbol{B} = \mu_0 \boldsymbol{H}$), M is the magnetic moment, B_r is the residual flux density of the magnet, and V is the volume of the magnet.

The coil's and magnet's forces F_{Coil} and F_{Magnet} acting on the model are represented as equations (10) and (11) respectively.

$$F_{\text{Coil}} = I \frac{0.15\times10^{-3}\, z}{(\sqrt{0.08^2 + z^2})^5} \qquad (10)$$

$$F_{\text{Magnet}} = \frac{9.93\times10^{-3}\, z}{(\sqrt{0.09^2 + z^2})^5} \qquad (11)$$

where I is a coil current and z is the distance from the coil or permanent magnet.

2.3.3 Measuring the flux density

Based on the analyzing method mentioned before, we estimated the flux density of each of the air-core coil and permanent magnet as well as the force exerted on the model. Tables 1 to 3 show the specifications of the coil, magnet, and model respectively. Figure 5 indicates the theoretical model of the air-core coil. We used the software MATHEMATICA for this calculation. Figure 6 and Figure 7 show the results and illustrate that the theoretical values agree with the measured ones.

Table1 Specification of the coil

Dimensions (Outer dia.× Inner dia.× Height)	180×140×30 [mm]
Wire diameter	ϕ 1.3[mm]
Number of turns	225

Table2 Specification of the magnet for the equipment

Dimensions (Outer dia.× Inner dia. × Height)	150×50×25 [mm]
Material	Neodymium (rare earth metal)
Residual flux density	1.39 [T]

Table3 Specification of the floating model

Shape and dimensions		Sphere 80[mm] in diameter
Volume		268[cm^3]
Total mass of floating model		700[g]
Material (outer housing)		Duracon^R
Magnet in floating model	Shape and dimensions	Column 40[mm]in dia. × 40[mm]high
	Material	Neodymium
	Residual flux density	1.39[T]

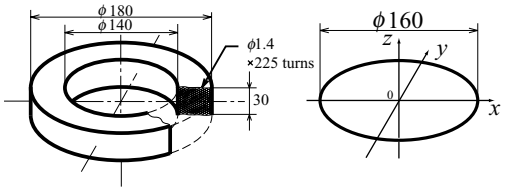

(a) Coil (b) Equivalent model

Figure 5: Analysis model in the simulation

Note that we regarded the permanent magnet as a coil through which a constant current flowed to give it an appropriate shape and current so that the calculation results agreed with the measured values. The magnetic force of the magnet shown in Figure 8, was derived theoretically. The mass of the floating model used for this experiment was 700 g, therefore the gravity acting on the model was 6.86 N. The equivalent magnetic force was given 0.166mm apart from the center of the permanent magnet as shown in Figure 8. The distance was equal to the actual floating position of the model.

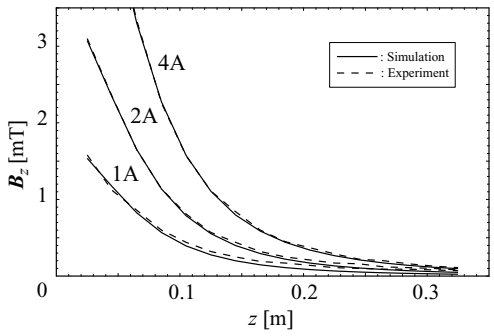

Figure 6: $\boldsymbol{B}_z$ (Coil, $x = 0$)

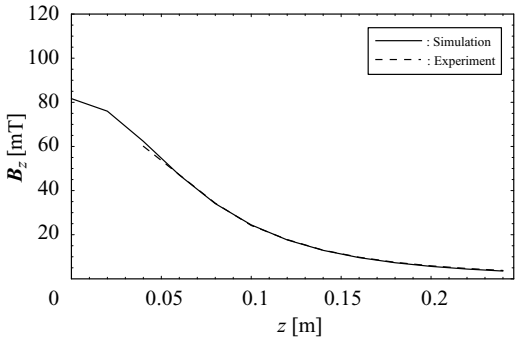

Figure 7: $\boldsymbol{B}_z$ (Magnet, $x = 0$)

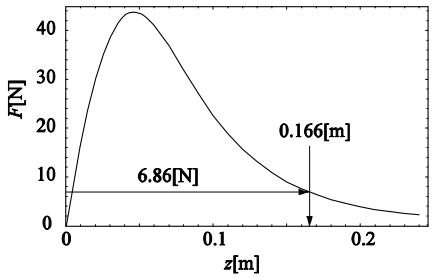

Figure 8: Magnetic force(Magnet, $x = 0$)

3. THE METHOD OF IDENTIFICATION OF THE DYNAMIC COEFFICIENTS

3.1 Block diagram of the 1DOF system

This subsection describes the measurement of the dynamic characteristics of a single-degree-of-freedom system and the effect of fluid-induced forces. Figure 9 illustrates an example of the system, and m, z, E, and H are the mass of the floating model, the displacement, the input signal (excitation), and the effect of fluid-induced forces acting on the model to be controlled, respectively. We identified each parameter of H by measuring the open-loop transfer function of the system.

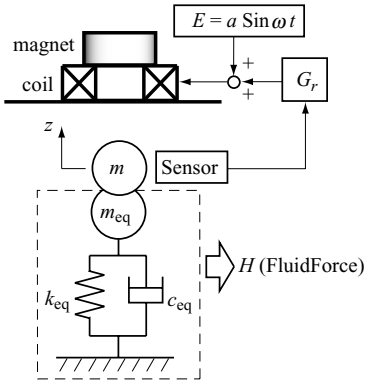

Figure 9: 1DOF model

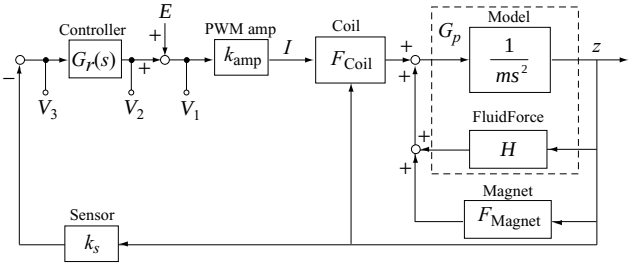

Figure 10: Measuring system of NDA-MSBS (1DOF)

Figure 10 is the block diagram of this measuring system. The equation of motion of the model is shown below:

$$m\ddot{z} + H = F_{\mathrm{Coil}}(I, z) + F_{\mathrm{Magnet}}(z) \qquad (12)$$

$$I = (k_s Gr(s) z + E) k_{\mathrm{Amp}} \qquad (13)$$

$$H = m_{eq}\ddot{z} + c_{eq}\dot{z} + k_{eq} z \qquad (14)$$

where F_{Coil} is the magnetic force of the coils, F_{Magnet} is the magnetic force of the permanent magnets, I is current, k_s is the sensor gain, k_{Amp} is the gain of PWM amplifier, $G_r(s)$ is the controller transfer function, m_{eq} is the added mass, c_{eq} is the equivalent damping coefficient, and k_{eq} is the equivalent spring constant. The open-loop transfer function is represented by the following equation:

$$G_o = -V_2/V_1 \qquad (15)$$

In the case of simulation we solved equations (12) - (14) and derived the open-loop characteristics from equation (15). In the case of experiments we measured V_1 and V_2, and the open-loop transfer function is obtained by FFT analyzer.

3.2 Identification of fluid dynamic coefficients

The fluid dynamic coefficients are identified by the following steps:

(a) [Simulation] In the case of $H = 0$, equations (12) - (14) is solved, and the open-loop transfer function is derived from equation (15).
(b) [Experiment] In the case of $H = 0$ (in air), the open loop transfer function is measured.
(c) Two transfer functions of (a) and (b) are compared, and the agreement of the results is confirmed. Therefore F_{Coil}, F_{Magnet}, and etc in equation (12) - (14) is correct.
(d) [Experiment] In the case of $H \neq 0$ (in fluid), the open loop transfer function is measured.
(e) [Simulation] By tuning the dynamic coefficients of H in simulations, the dynamic coefficients are estimated.
(f) Two transfer functions of (d) and (e) are compared, and the agreement of the results is confirmed. Therefore the dynamic coefficients are identified.

3.3 Confirmation experiments

We conducted two kinds of experiments in air. We used a spherical body with an 80mm diameter as the model.

3.3.1 Excitation test in air ($H = 0$) (step a, b, c)

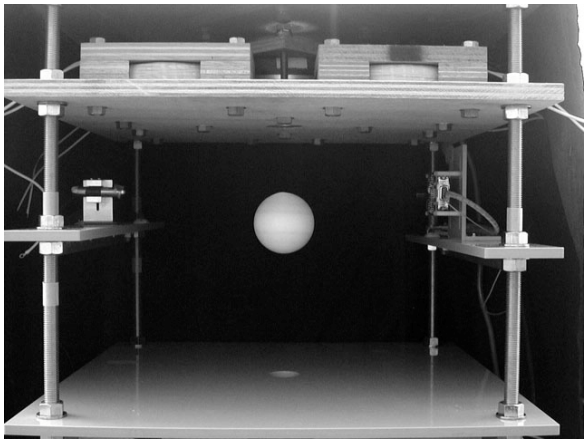

Figure 11: Photograph of the floating model in air ($m_{eq} = 0$)

We conducted an excitation test in air. Figure 11 shows the model being levitated in air. It is 160mm apart from the equipment's permanent magnet.

Figure 12 presents results from the simulation and measurement of the open loop transfer function. The measured and simulated results are shown by solid and dashed lines, respectively. We carried out the simulation. Assuming that the viscosity of the air can be ignored, that is $H = 0$, because the excitation amplitude is very small. The figure shows that the simulated values closely agree with the measured values.

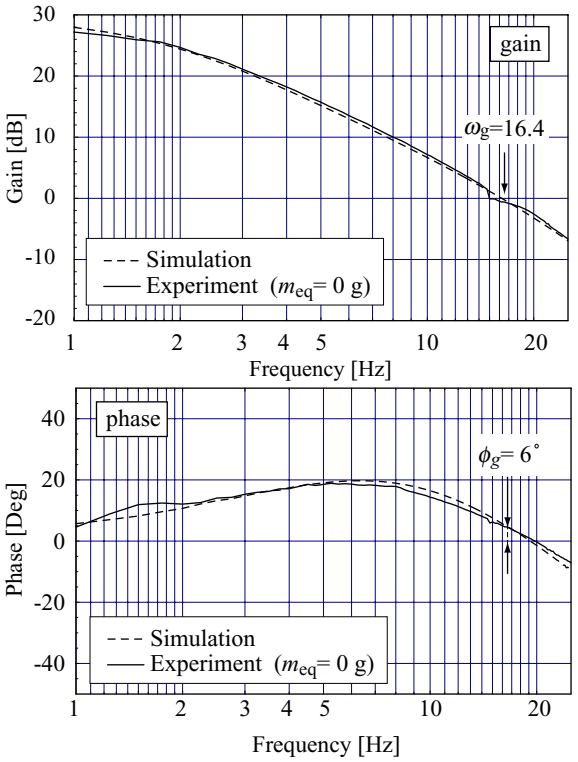

Figure 12: Open loop transfer function (in air, $m_{eq} = 0$)

3.3.2 Excitation test with a weight (m_{eq} = 30 g) added (step d, e, f)

Next, we added a weight of 30 grams to the model and conducted the excitation test to check whether we can simulate the external effects on the model. Figure 13 shows the resulting open-loop transfer functions. The thick, solid, and dashed lines refer to the measurement with $m_{eq} = 0$, the measurement with $m_{eq} = 30$ g, and the simulation with $m_{eq} = 30$ g, respectively. Comparing the two experimental results indicate that the gain plots are equally apart from each other, which means the effect of the weight added to the model.

In the case of $m_{eq} = 30$ g, a comparison of the measured and simulated values indicates that both plots are very consistent with each other, as is shown by the results with no weight. Therefore, H estimated by this experiment is written as the following equation:

$$H = 0.03\ddot{z} \qquad (16)$$

The results obtained in the previous subsection and in this one suggest that our simulator can correctly represent changes in the dynamic coefficients derived from the varying states of the model.

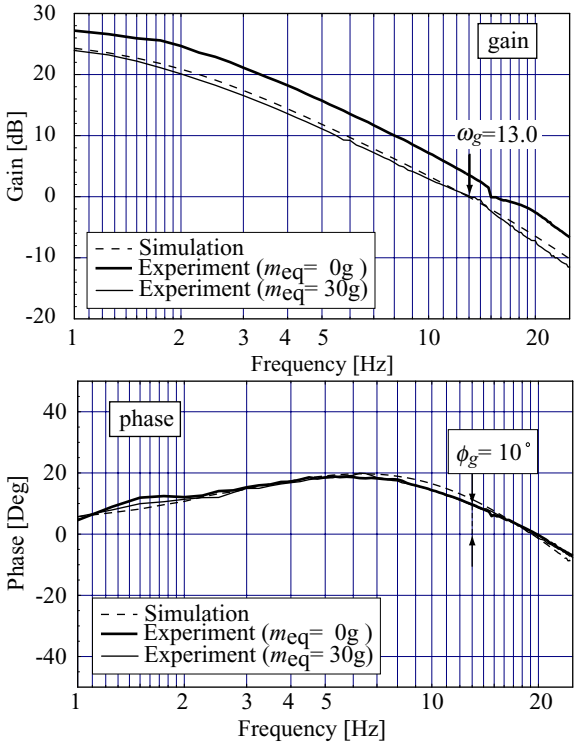

Figure 13: Open loop transfer function (in air, $m_{eq} = 30g$)

4. MEASURING THE DYNAMIC COEFFICIENTS

In the same manner as the previous section, we also excited the model in water to measure the dynamic coefficients of the model affected by the water. In order to avoid friction between the water and tank walls as well as the influence of water convection, we used an acrylic water tank 350mm high, 35mm wide, and 790mm deep. Moreover, to eliminate any free interface and air in the tank, we used a lid to hermetically seal the tank. Figure 15 shows the photograph of the experimental system with the water tank, and Figure 16 shows the model suspended in the water.

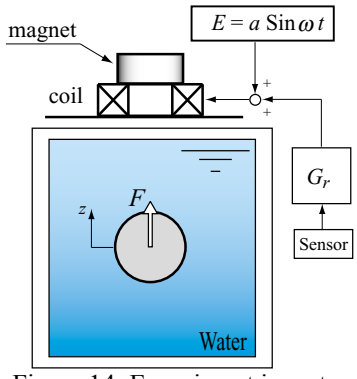

Figure 14: Experiment in water

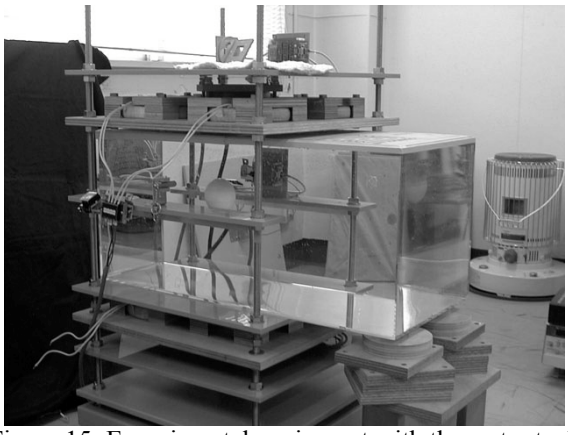

Figure 15: Experimental equipment with the water tank

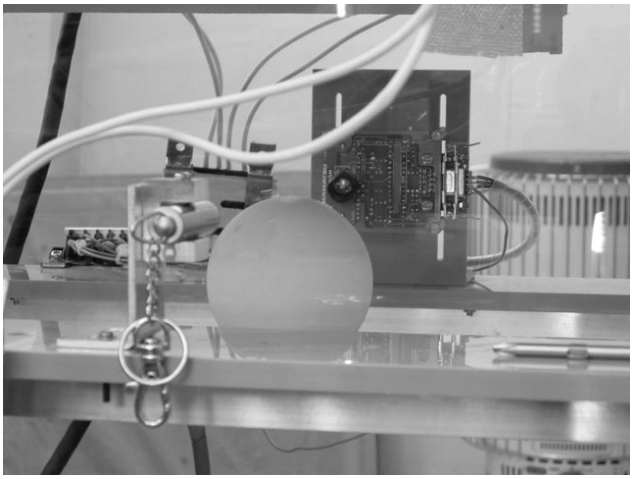

Figure 16: The model floating in water

Figure 17 presents the measured and simulated gain and phase plots. The H parameter is adjusted so that both plots are consistent with each other. The solid, thin dashed, and dashed thick lines represent the measurements in water, the simulation with $H = 0$, and the simulation with estimated H. Based on the results, H estimated by this experiment is written as the following equation:

$$H = 0.2m\ddot{z} - 0.5\dot{z} \qquad (17)$$

where m is the mass of the model (700 grams). Letting V and ρ be the volume of the sphere (m^3) and the density of the water (kg/m^3) respectively, the influence of the added mass of equation (17) is written as follows:

$$0.2m \cong 0.5\rho V \qquad (18)$$

This value is almost the same as the one specified in general reference guides[8].

5. CONCLUSION

We have confirmed the effectiveness of a method for clarifying the effect of fluid-induced forces on the dynamic coefficients of the model by comparing the measured and simulated open-loop transfer functions. However, for parameters other than the added mass, we have no data for directly comparing the dynamic coefficients, therefore, in the future we must establish a way to verify the method's correctness.

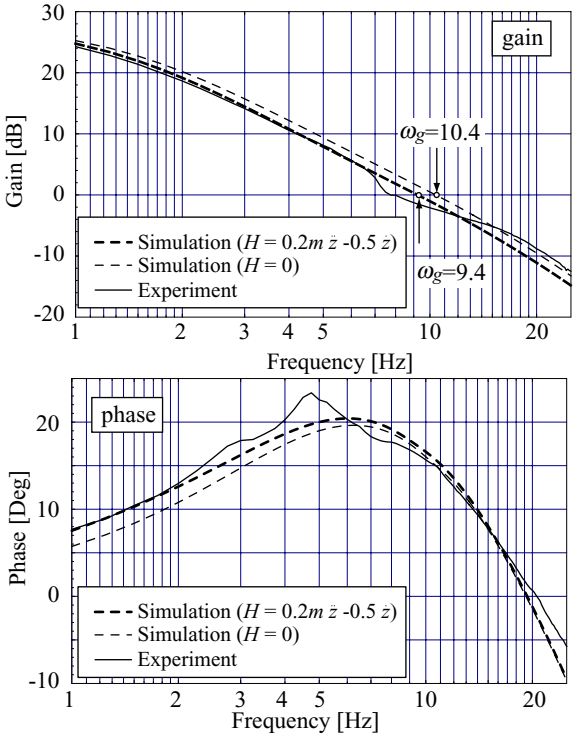

Figure 17: Bode plot (in water)

[1] E.E.Covert, Magnetic Suspension and Balance System IEEE AES Magazine, pp.14, May 1988

[2] T.S.Daniels, J.S.Tripp, Improvements to an Electromagnetic Suspension Wind Tunnel, Proc. International Instrumentation Symposium, 34, pp.65-70, 1988

[3] P.Tcheng, T.D.Schott, E.L.Bryant, A Miniature, Infrared Pressure Telemetry System, Proc. of International Instrumentation Symposium, 34, pp.407-416, 1988

[4] C.P.Britcher, Electromagnet Configurations for Extreme Attitude Testing in Magnetic Suspension and Balance Systems, Semiannual Progress Rept., period ending December 1980, NASA CR-163862, pp.22, May 1981

[6] Hideo Sawada, Tetsuya Kunimasu, Status of MSBS Study at NAL, 6th International Symposium on Magnetic Suspension Technology, 2001

[7] Yoshiyuki Kawamura, Wind Tunnel Experiments Using a Low-Electric Power 40cm-Class Magnetic Suspension and Balance System in Fukuoka Institute of Technology, Flow Vol.22, pp. 309-315, 2003 (In Japanese)

[8] JSME Mechanical Engineers' Handbook, A5, pp.129-130, 2001 (In Japanese)